



Pore Pressure Prediction Using Velocity-Mean Effective Stress Relationship in Madura Sub-basin, East Java Basin - Indonesia

SENA W. REKSALEGORA¹, LAMBOK M. HUTASOIT¹, AGUS H. HARSOLUMAKSO¹, AND AGUS M. RAMDHAN¹

¹Department of Geology, Institute of Technology Bandung, Bandung 40132, West Java, Indonesia

Corresponding author: sena.reksalegora@gmail.com
Manuscript received: February, 9, 2020; revised: June, 6, 2020;
approved: December, 20, 2021; available online: July, 8, 2022

Abstract -Pore pressure prediction using velocity-mean effective stress relationship is introduced in Madura Subbasin which is located in a compressional tectonic setting. The new workflow accommodates the three principal stresses, those are vertical stress, maximum horizontal stress, and minimum horizontal stress in a form of mean stress as the compaction main inducing agent. The application of this new workflow has resulted in a more accurate pore pressure prediction where the normally used pore pressure prediction method tends to underestimate the actual data. In Dukuh-1 well, as an example, the pore pressure prediction from the new work flow is able to explain the continuous hole problems such as well flows and well kicks that were recorded during drilling. In MDA-2 well, the new pore pressure prediction closely matches the well data in comparison to the normally used prediction. As a result, a more accurate regional pore pressure prediction map using mean stress is generated to aid both hydrocarbon exploration and development activities in the study area.

Keywords: compressional tectonic setting, pore pressure prediction, vertical stress, minimum horizontal stress, maximum horizontal stress, mean stress, mean effective stress, compaction main inducing agent

© IJOG - 2022

How to cite this article:

Reksalegora, S.W., Hutasoit, L.M., Harsolumakso, A.H., and Ramdhan, M.R., 2022. Pore Pressure Prediction Using Velocity-Mean Effective Stress Relationship in Madura Sub-basin, East Java Basin - Indonesia. *Indonesian Journal on Geoscience*, 9 (2), p.247-262. DOI: [10.17014/ijog.9.2.247-262](https://doi.org/10.17014/ijog.9.2.247-262)

INTRODUCTION

Background

The study area is located in Madura Sub-basin of East Java Basin which is one of hydrocarbon producing basins in Indonesia (Figure 1). Small and shallow oil and gas accumulations are common on onshore areas, while medium size gas accumulations are discovered in offshore areas. The study area is part of worldwide area where pore pressure is affected by tectonic processes (Yassir and Addis, 2002).

The tectonic evolution of the East Java Basin is primarily controlled by compressional tecto-

nism due to the northward convergence of the Australian Plate and Sundaland margin (Sribudiyani *et al.*, 2003). Two principal structural trends are present in the East Java Basin: east-west strike-slip fault, known as the Sakala trend and northeast-southwest Meratus extensional fault trend. The study area is dominated by the east-west strike-slip fault Sakala trend.

The dominant sediment fills of East Java Basin are the mixed of carbonate and clastic sediments of marine origin. The carbonate and clastic progradation were developed during relative highstands, while during major lowstand, clastic sediments dominated the area and carbon-

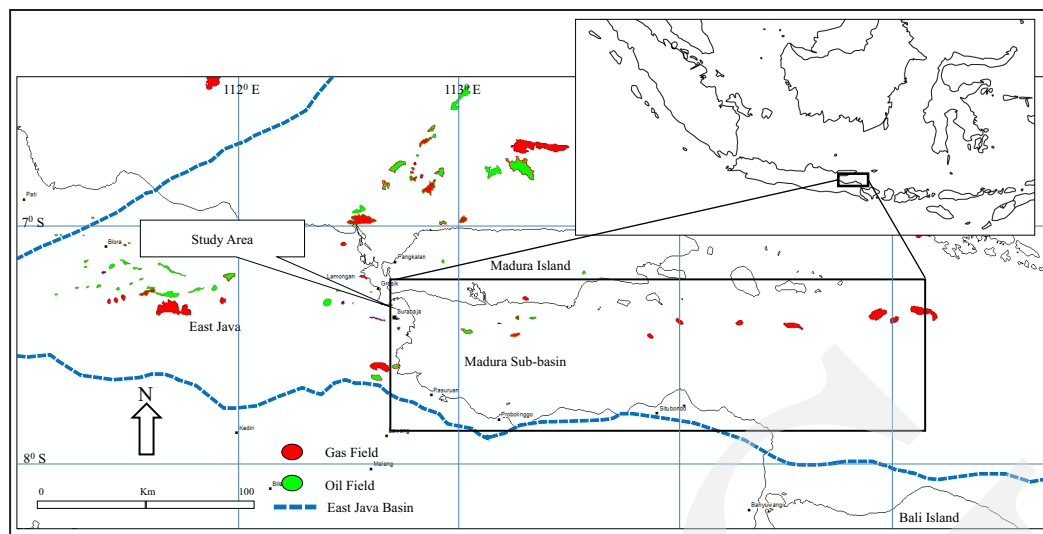


Figure 1. Madura Sub-basin is located in the southern part of East Java Basin.

ate development halted. The transgressive period was responded by reefal limestone development (Brandsen and Matthews, 1992).

This paper discusses the new workflow in pore pressure prediction that takes into account the three-dimensional nature of the stress field. This method is well tested in this compressional tectonic setting. It accommodates the three principal stresses, those are vertical stress, maximum horizontal stress, and minimum horizontal stress in a form of mean stress as the compaction main inducing agent. Normally, the used pore pressure prediction in the study area considers only overburden or vertical stress as one dimensional compaction main inducing agent (Manik and Soedaldjo, 1984; Kusumastuti *et al.*, 1999; Tanikawa *et al.*, 2010; Ramdhan *et al.*, 2011; Ramdhan *et al.*, 2013; Hutasoit and Ramdhan, 2014; Tingay, 2015). The application of this new work flow has resulted in a more accurate pore pressure prediction.

The following section start with a short review of East Java Basin geology and a brief description of the data used. The rest of the section concentrates on the description of the method and data. Short discussion is presented at the last part of the paper.

Geologic Setting

The East Java Basin was originally part of northern Australia that was shifted north started

at 155 Mya (Metcalf, 2013; Zahirovic *et al.*, 2014). This basin was subjected to north-south compressional tectonic since Early Miocene as a result of the subduction of the Indo-Australian Plate under the Micro Sunda Plate (Sribudiyani *et al.*, 2003). The present day orientation of regional compressional stress in the study area is in NNE-SSW direction (Magee *et al.*, 2010; Heidbach *et al.*, 2016).

Physiographically, the study area is part of Kendeng and Rembang Zones (Bemmelen, 1949). The Madura Sub-basin is the continuation of the onshore Randublatung depression of Rembang Zone, Kendeng Hills of Kendeng Zone and Central Plain of East Java (Figure 2). During Plio-Pleistocene, the Kendeng Zone experienced a strong deformation with decreasing intensity from onshore to the study area (Genevraye and Samuel, 1972).

The East Java Basin stratigraphic naming varies from onshore to offshore areas as summarized by Pertamina BPKKA (1996, Figure 3). The stratigraphy of the study areas reflects the balance between carbonate and clastic sediment deposited in a marine environment. The primary hydrocarbon exploration target in the Madura Sub-basin consists of Pliocene GL Formation as the shallow target and Miocene Kujung Formation as the deeper target. The oldest formation penetrated in the study area is the upper Ngim-

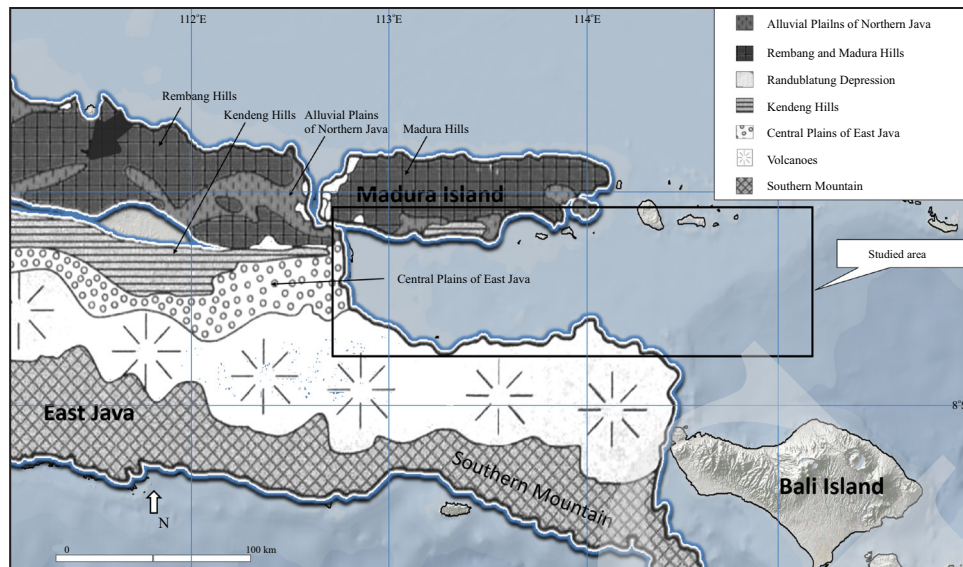


Figure 2. The study area is the offshore continuation of Rembang and Madura hills in the northern part and a combination of Randublatung depression, Kendeng Hills and central plains of East Java in the southern part (Bemmelen, 1949).


Age	Onshore								Offshore	
Pleistocene	Lidah +MT									
Pliocene	Kawengan		GL		Upper Karen		Paciran			Mundu
Miocene	OK	Upper OK	Wonocolo		Lower Karen		Cepu	Upper Cepu	Cepu	
		Lower OK	Tawun		Tuban		Rancak	Lower Cepu		
Oligocene	Kujung	Kujung I	Kujung Carbonate		North Madura Platform	Kranji	Upper Prupuh		Prupuh	
		Kujung II					Lower Prupuh			
		Kujung III	Kujung Shale			CD	Poleng			
Eocene	Pre Kujung	Pre CD		Ngimbang	Ngimbang Shale					
					Ngimbang Carbonate					
					Ngimbang Clastic					
Cretaceous						Pre Ngimbang				
						Basement				

Figure 3. East Java Basin generalized stratigraphic framework, simplified from Pertamina BPPKA (1996). The stratigraphic nomenclature varies from onshore to offshore. The primary target in the study area is the Pliocene GL limestone as the shallow target and Oligocene to Lower Miocene Kujung limestone as the deeper target. Blue is carbonate, yellow is sandstone, and dark red is basement which is either metamorphic or igneous rock.

bang Formation at MCD-1 well with a total depth of 4,852 m TVDSS.

METHOD

The commonly used method for pore pressure prediction in shale is Eaton method (Eaton, 1975) which was developed using numerous Gulf

Mexico overpressure wells in tectonically relaxed area dominated by normal fault stress regime (Yassir and Zerwer, 1997). His method considers vertical stress as the compaction main inducing agent as shown in the following Eaton empirical relationship for sonic log:

$$P = \sigma_v - (\sigma_v - P_n) \left(\frac{\Delta t_n}{\Delta t} \right) \dots \dots \dots (1)$$

where:

P is pore pressure;

σ_v is vertical stress;

P_n is hydrostatic pressure;

Δt_n is normal trend transit time;

Δt is log transit time with units for pressure and stress in MPa and second/foot for transit time.

However, it is noted that the application of this Eaton empirical relationship in other Tertiary basins in the world with different stress regime requires adjustment to its standard exponential value. As an example, to generate pore pressure prediction using Eaton empirical relationship for sonic log in inner shelf Baram Delta, Brunei Darussalam, the best exponential value to fit the data is 6.5 instead of standard exponential value of 3 (Tingay, 2003).

This paper offers a pore prediction work flow using velocity-mean effective stress relationship that is suitable to the study area which it is located in a compressional tectonic setting. The magnitude of mean effective stress is derived from direct application of Terzaghi principle (Terzaghi, 1925) by subtracting the mean stress with the pore pressure collected from well direct and indirect pressure measurements. The mean stress substitutes the vertical stress as the main compaction inducing agent:

$$\text{Mean effective stress} = \text{Mean stress} - \text{Pore pressure} \dots (2)$$

RESULT AND DATA

Data from twenty-four exploratory wells and approximately 5,900 km of offshore 2D seismic vintage 1968-1998 which consist of SEG Y and navigation data are used in this study (Figure 4). The wells were drilled in the period of 1970 to 2012 by twelve different operators. The well data consist of logs, drilling report, well completion report, mudlog, borehole temperature, direct pressure measurement (Repeat Formation Tester (RFT), Modular Dynamic Tester (MDT), Drill Stem Test (DST), Leak Off Test (LOT), Formation Integrity Test (FIT)), indirect pressure measurement (Mud Weight (MW)), well velocity {checkshot, Vertical Seismic Profile (VSP)}, petrography, sedimentology, geochemical analysis report, and biostratigraphy analysis report (Table 1). All wells were drilled to at least the depth below top of overpressure.

Data Processing

Subsurface Mapping

By using 2D offshore seismic data, six seismic horizons were mapped. The seismic data recorded well the effect of compressional tectonic as displayed in one of the seismic lines in the western part of the study area (Figure 5). Available well Vertical Seismic Profile (VSP) and checkshot data are used to generate time to depth function for converting time structure map to depth structure

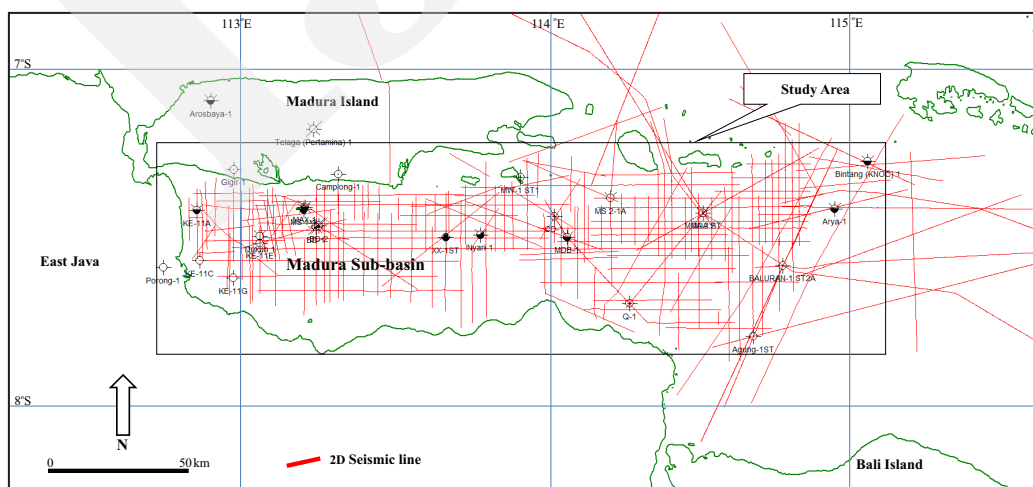


Figure 4. Distribution of the data used in this study: well (black circle), 2D seismic (red line).

Table 1. A Total of Twenty-four Exploratory Wells with Sufficient Data are incorporated in this Study. The total depth for each well is in meter subsea with MCD-1 Well as the deepest well

No	Well Name	TD TVDSS meter	Logs				VSP/ Check-shot	Direct Pressure Measurement			Report		
			GR	Resistivity	Density	Sonic		DST	RFT, MDT	LOT /FIT	Biostratigraphy	Geo-chemistry	Petro-graphy
1	Agung-1	2181	x	x	x	x				x		x	
2	Arosbaya-1	2771	x	x	x	x	x	x		x	x	x	
3	Arya-1	3028	x	x	x	x	x				x	x	x
4	Baluran-1	4150	x	x	x	x	x			x	x	x	x
5	Bintang-1	2515	x	x	x	x	x		x	x	x	x	x
6	Camplong-1	1544	x	x	x	x				x	x		
7	Dukuh-1	2659	x	x	x	x				x	x	x	x
8	Gigir-1	2840	x	x	x	x					x	x	
9	KE-11A	1202	x	x	x	x	x	x			x	x	x
10	KE-11C	3027	x	x	x	x	x	x			x	x	
11	KE-11E	4704	x	x	x	x	x	x		x	x	x	
12	KE-11G	4712	x	x		x							
13	MDA-2	1512	x	x	x	x	x	x		x	x	x	x
14	MDB-1	1371	x	x	x	x	x		x	x	x	x	x
15	MBD-1	4256	x	x	x	x	x	x		x	x	x	x
16	MBD-2	3474	x	x	x	x	x	x		x	x	x	x
17	MCD-1	4852	x	x	x		x	x		x	x	x	x
18	MW-1	3915	x	x	x	x	x		x	x	x	x	x
19	Q-1	3352	x	x	x	x	x			x	x	x	x
20	MSI-1	2640	x	x	x	x				x	x	x	
21	MSI-2	3133	x	x	x	x				x	x	x	
22	XX-1	4376	x	x	x	x	x	x		x	x	x	x
23	Nyari-1	3447	x	x	x	x	x		x	x	x	x	x
24	Telaga-1	3108	x	x	x	x	x	x		x	x	x	x

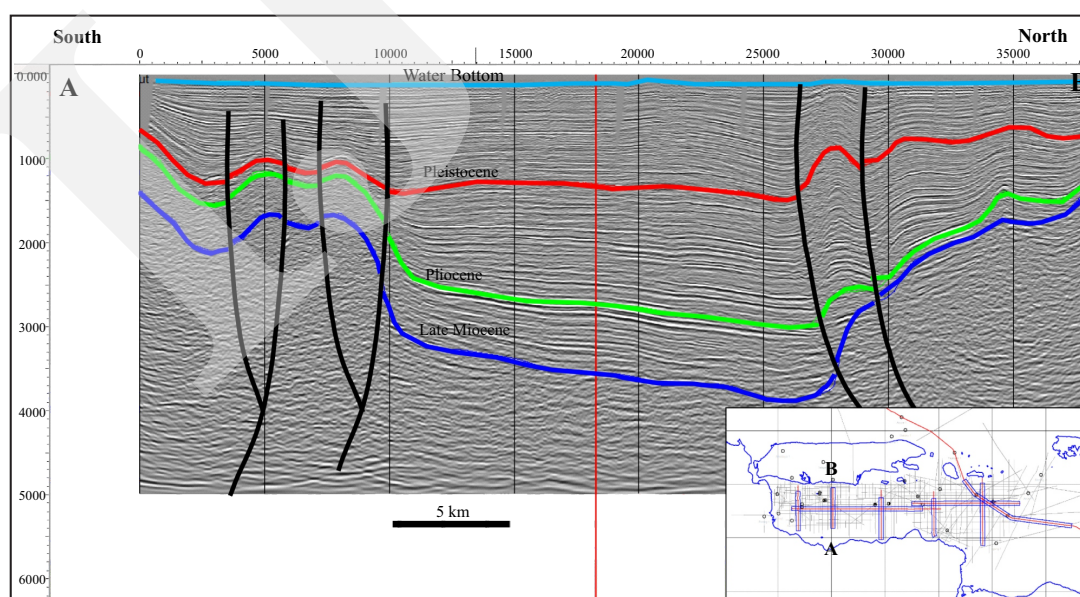


Figure 5. South-North seismic line (A to B) in the western part of the studied area illustrates the present day structural configuration as the result of the NNE-SSW direction of regional compressional stress. Folds and thrust faults concentrate in the northern and southern part of the studied area.

map. Well corrected Pleistocene horizon depth structure map shows general structure of the study area, which consists of elongated highs in both the northern and southern areas with lows in the middle part (Figure 6).

Vertical Stress Magnitude Estimation

The magnitude of vertical stress (S_v) is the stress exerted from the weight of the overburden above a point of measurement (Bell, 1996; Engelder, 1993; Jaeger *et al.*, 2007). The magnitude of vertical stress for onshore location is calculated using the following formula:

$$S_v = (z) g z \dots\dots\dots (3)$$

The magnitude of vertical stress for offshore location is corrected for water depth as below:

$$S_v = \rho_w g z_w + (z) g z \dots\dots\dots (4)$$

where:

S_v is overburden/vertical stress;

$\rho(z)$ is rock density as a function of depth;

g is gravitational force;

ρ_w is water density;

Z is depth;

Z_w is water depth with units for stress in MPa,

density in g/cm^3 ,

gravity in m/second^2 ,

depth in m.

The rock density magnitudes come from density log, sonic log, and VSP. The available density log went through conditioning process from borehole correction to density averaging. Density readings that are not representing the actual rock density were removed. In the shallow section, density is not normally logged, mainly because the section commonly is not the primary target. In the absence of density log, Gardner sonic velocity (V_p) to density (ρ) transform was utilized to estimate the density from the surface to the top of the density log (Gardner *et al.*, 1974). The following function is Gardner transformation derived for sedimentary rocks and is valid for $1.5 < V_p < 6.1$ km/second:

$$\rho = 1.741 V_p^{0.25} \dots\dots\dots (6)$$

Gardner transformation needs approximately 0.15 g/cm^3 adjustment to get the best fit in a well location in the study area. The density logs were extrapolated from the top of the log to sea bottom for offshore wells or ground level for onshore wells in the absence of sonic velocity data.

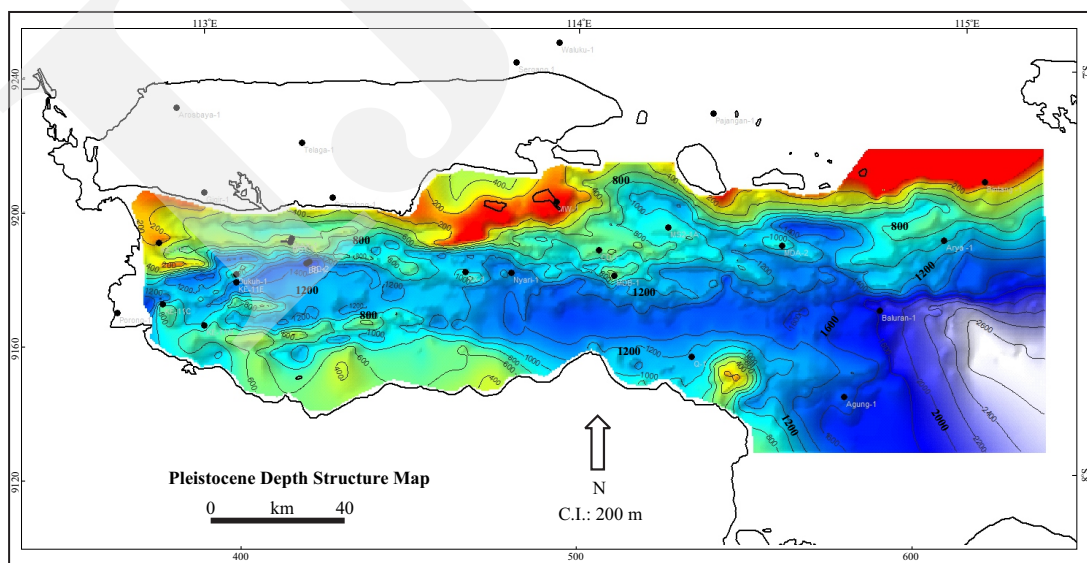


Figure 6. Well corrected depth structure map of Pleistocene horizon shows west-east elongated anticlinal structure with highs (red) in the north and southern part of the studied area and lows in the middle part (blue to light blue). Pleistocene horizon is outcropping in the northern side of the studied area.

The magnitude of vertical stress varies vertically with depth as well as laterally between wells. A well corrected vertical stress map of Pleistocene horizon is generated using relationship of vertical stress as a function of depth (Figure 7). The vertical stress magnitude lateral distribution follows the Pleistocene structural trend with high magnitude concentrates in the middle part and increases from west to east and it is a function of sediment thickness above it (Figure 8).

Horizontal Stress Magnitude Estimation

The magnitude of minimum horizontal stress (S_{hmin}) is obtained from well Leak Off Test (LOT) and Formation Integrity Test (FIT) data (Bell, 1996; Zoback, 2007). A relationship of minimum horizontal stress as a function of depth is developed (Figure 9). A well corrected minimum horizontal stress magnitude map of Pleistocene horizon is generated (Figure 10).

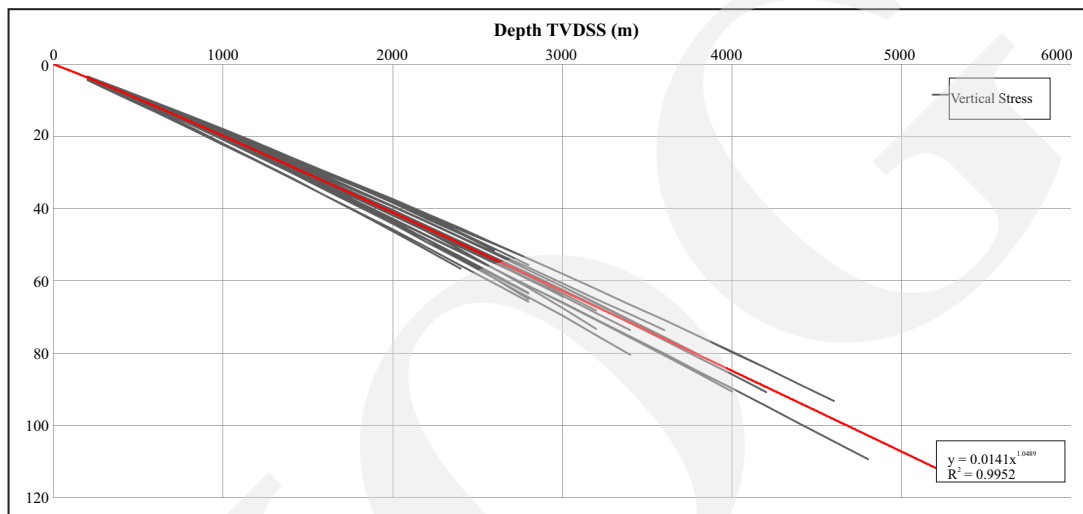


Figure 7. Relationship of vertical stress as a function of depth of all wells with available data is excellent with correlation coefficient of > 0.9 .

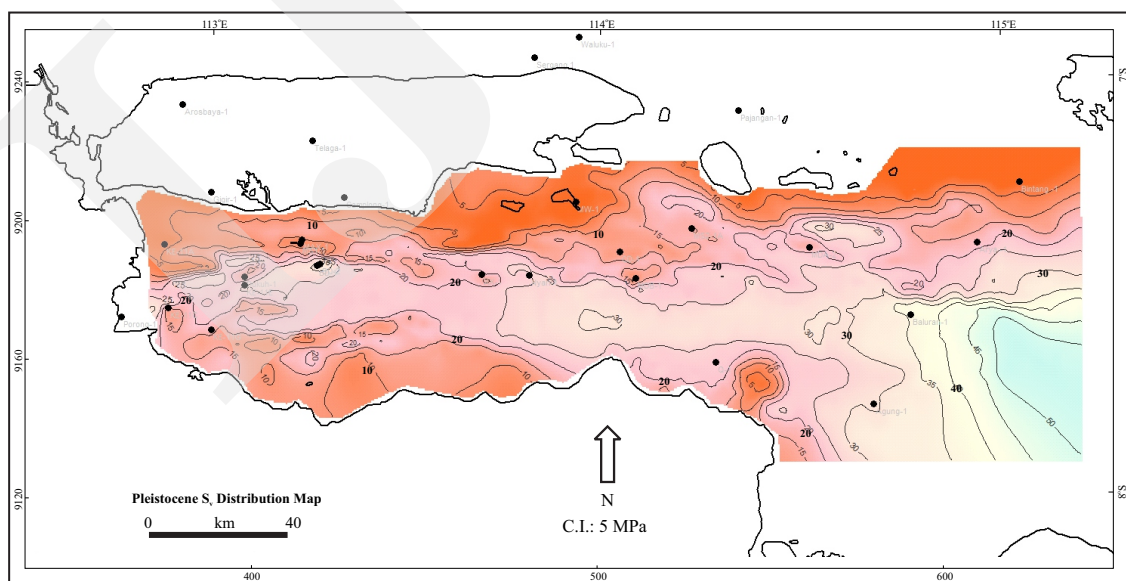


Figure 8. Vertical stress distribution map for Pleistocene horizon generally follows the structure of the same horizon. The magnitude ranges from ≥ 0 MPa where the horizon basically exposed in the northern part (red) to magnitude > 50 MPa in the eastern part of the studied area which is a structurally low area (light blue). High magnitude trend in the middle part of the studied area reflects thicker sediments.

The magnitude of maximum horizontal stress (S_{Hmax}) is the most difficult principal stress to estimate. This study incorporates frictional faulting theory where the ratio of the main principle effective stress (σ_1') and the minimum principle effective stress (σ_3') is a function of rock coefficient friction (μ) (Jaeger *et al.*, 2007), as shown below:

$$\sigma_1' / \sigma_3' = (S_1 - P_p) / (S_3 - P_p) = [(\mu + 1) / (2 + \mu)] = f(\mu) \dots\dots\dots (6)$$

Assuming rock coefficient friction = 0.6 for sediment shallower than 6 km (Byerlee, 1978) and strike-slip stress regime where the main principle

stress (S_1) is S_{Hmax} and the minimum principle stress (S_3) is S_{Hmin} , the frictional faulting theory becomes (Jaeger *et al.*, 2007):

$$S_{Hmax} = 3.1 S_{Hmin} - 2.1 P_p \dots\dots\dots (7)$$

Pore pressure (P_p) information was collected from both direct and indirect pressure measurements. All wells in this study are exploration wells with limited direct pressure measurement (DST, MDT, RFT). Indirect pressure measurement (MW) is incorporated with cautious as their reading are normally higher than the pore pressure

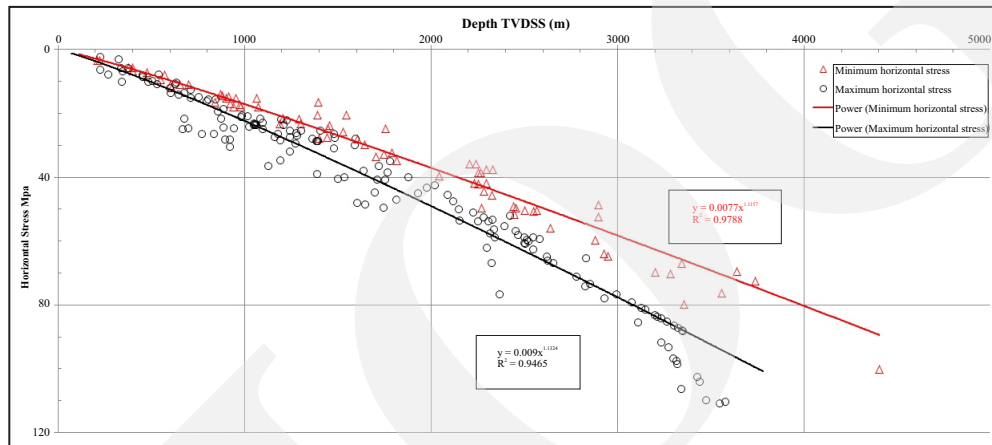


Figure 9. Relationship of both horizontal stresses (red triangles for S_{Hmin} and black circle for S_{Hmax}) as a function of depth of all wells with available direct and indirect pressure measurement is excellent with correlation coefficient of > 0.9.

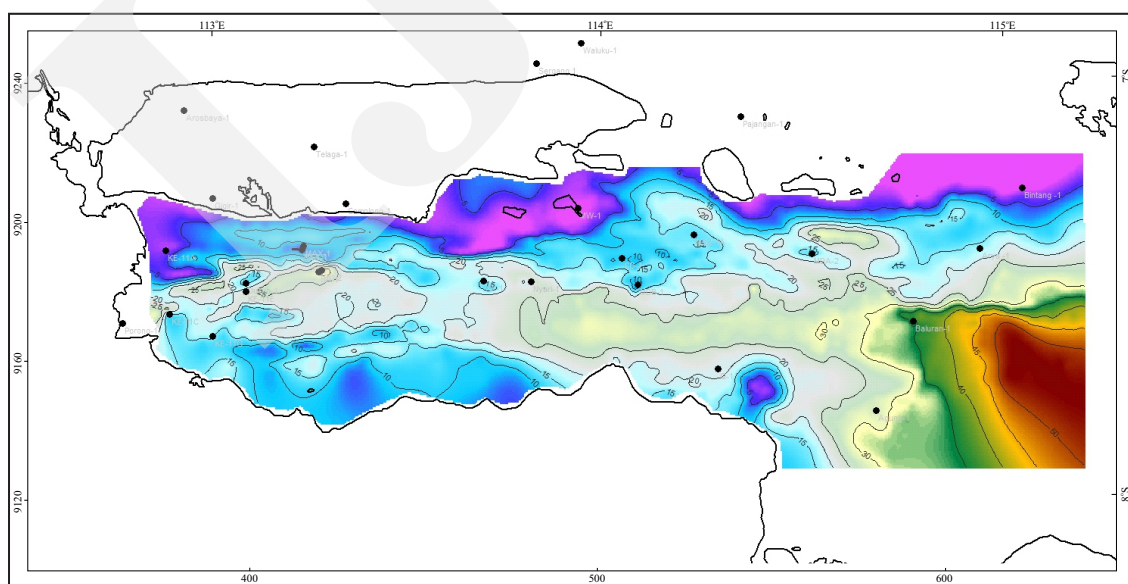


Figure 10. Minimum horizontal stress magnitude distribution map for Pleistocene horizon generally follows the structure of the same horizon. The overall magnitude is slightly less than the vertical stress in a regional scale.

(Ruth *et al.*, 2000). Using limited pore pressure reading, the magnitude of maximum horizontal stress is estimated and its relationship as a function of depth for each well is generated (Figure 9). A well corrected maximum horizontal stress magnitude map of Pleistocene horizon is created using relationship of maximum horizontal stress as a function of depth (Figure 11).

Mean Stress, Mean Effective Stress, and Pore Pressure Prediction

Common pore pressure prediction method in sedimentary basins assumes only one dimensional compaction with overburden or vertical stress as the main inducing agent. Compaction is actually three dimensional (Traugott, 1997; Schutjens *et al.*, 2004). Therefore, horizontal stresses must be included in pore pressure prediction, especially in a compressional tectonic setting. While the general stress state for an area is represented by nine stresses component (Zoback, 2007). This study uses only the magnitude of the three principal stresses which are the maximum horizontal stress, the minimum horizontal stress, and the vertical stress to define the mean stress. Mean stress method has been exercised previously in pore pressure prediction, however with the as-

sumption that the magnitude of both horizontal stresses are equal (Harrold *et al.*, 1999; Ruth *et al.*, 2003). This study adopts the estimated magnitude of all three principal stresses:

$$\text{Mean stress} = 1/3 * (S_{H_{\max}} + S_{H_{\min}} + S_v) \dots\dots\dots (8)$$

The relationship of mean stress as a function of depth is developed (Figure 12) and a well corrected mean stress magnitude distribution map of Pleistocene horizon is generated using the relationship (Figure 13).

As mentioned earlier in the background of the study, the magnitude of mean effective stress is derived from direct application of Terzaghi principle (Terzaghi, 1925) by subtracting the mean stress with the pore pressure reading collected from well direct and indirect pressure measurement. The mean stress substitutes the vertical stress as the main compaction inducing agent.

A relationship of mean effective stress and sonic interval velocity is developed (Figure 14). In the well case, this relationship is simply multiplied with well sonic interval velocity to get the mean effective stress. In the regional case, seismic interval velocity substitutes the well sonic interval velocity. A well corrected mean effective

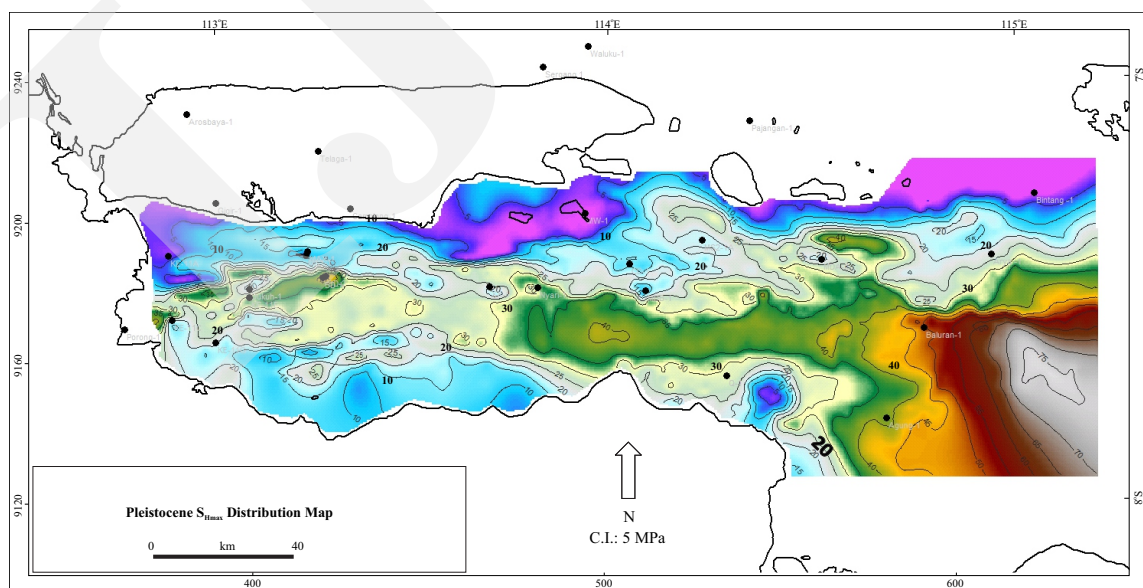


Figure 11. Maximum horizontal stress magnitude distribution map for Pleistocene horizon is identical with the minimum horizontal stress magnitude in the regional trend. However, the overall magnitude is higher than both the vertical stress and the minimum horizontal stress in a regional scale.

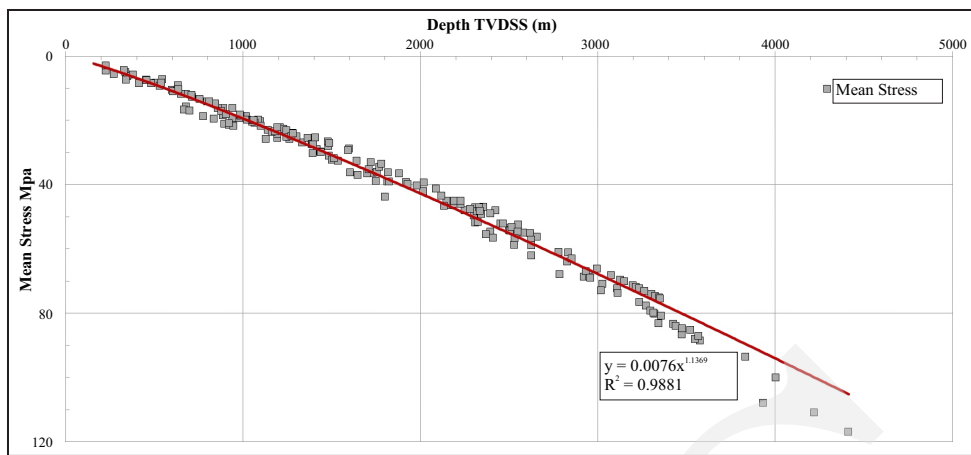


Figure 12. An excellent correlation coefficient of > 0.9 is achieved for the relationship of mean stress as a function of depth of all wells with available data.

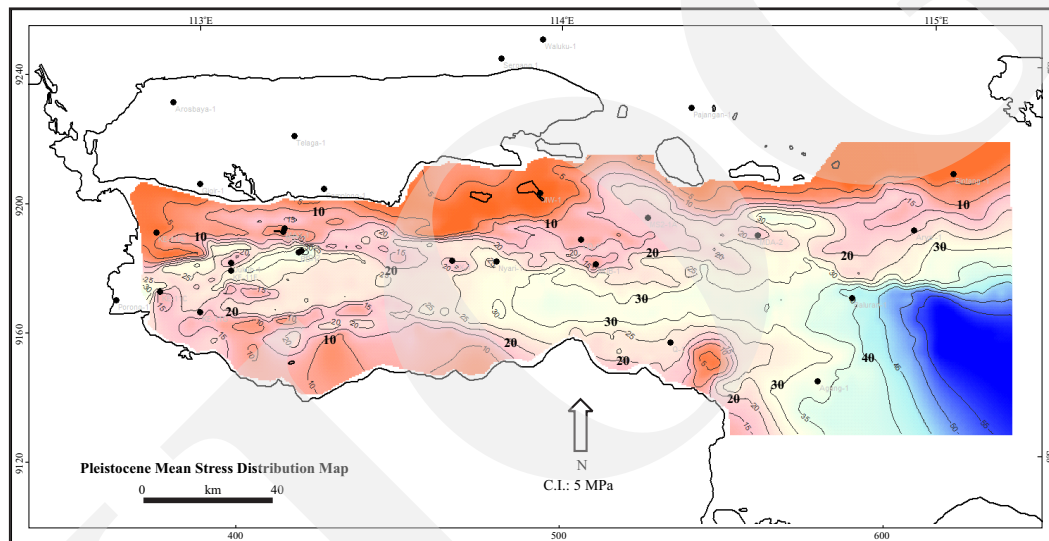


Figure 13. Mean stress distribution map for Pleistocene horizon. In general, the mean stress magnitude is higher than the vertical stress magnitude.

stress magnitude distribution map of Pleistocene horizon is generated using the relationship with seismic interval velocity (Figure 15). The regional pore pressure distribution for Pleistocene interval is then simply predicted by subtracting the regional Pleistocene mean stress with the regional Pleistocene mean effective stress.

DISCUSSION

Stress Regime

The subsurface stress condition is adapted from Anderson faulting theory (Anderson, 1951).

The present day Madura Island and the rest of the northern half of the study area is part of a the well-known west to east wrench zone, left-lateral slip in nature called Rembang-Madura-Kangean-Sakala (RMKS) fault zone (Satyana *et al.*, 2004). The Plio-Pleistocene interval has been eroded in the Madura Island and exposes the Miocene interval almost in the entire island (Ratman *et al.*, 1998). Knowing that the study area is subjected to compressional tectonic, the stress regime conclusion for the Pleistocene horizon is further supported by the ratio $S_{hmin}/S_v \leq 1$ (Figure 16) and $S_{Hmax}/S_v > 1$ (Figure 17) and confirms a strike-slip fault stress regime ($S_{Hmax} \geq S_v \geq S_{hmin}$).

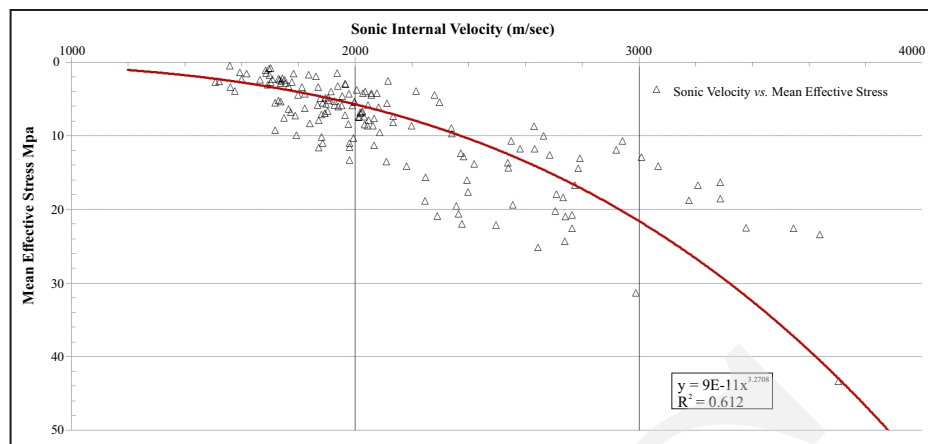


Figure 14. The relationship between mean effective stress and sonic interval velocity of all wells with direct and indirect pressure measurements. The coefficient correlation is > 0.6 which suggest fair correlation.

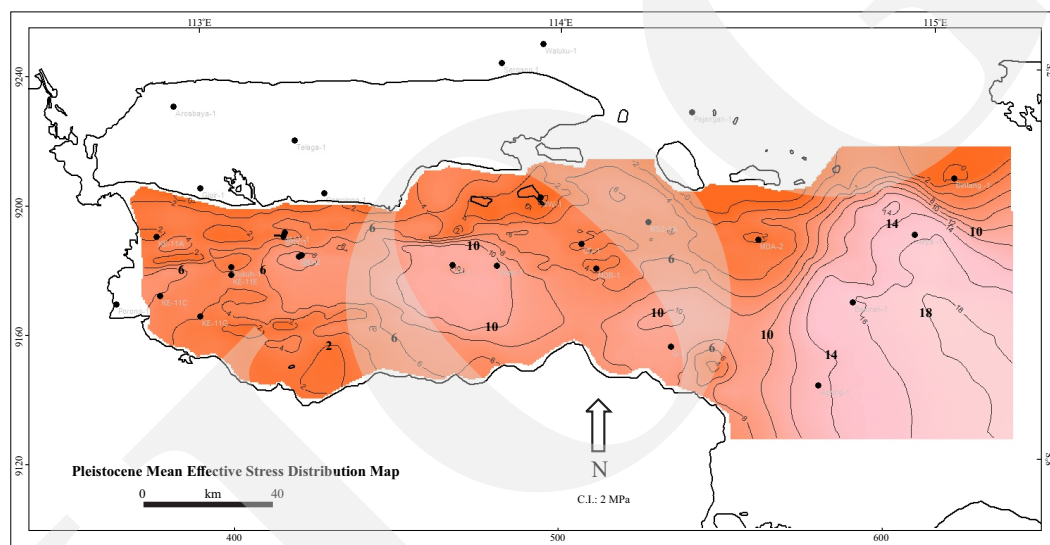


Figure 15. Mean effective stress distribution map for Pleistocene horizon. This map is generated using seismic interval velocity as the substitute of sonic interval velocity.

Pore Pressure Prediction

Pore pressure prediction using the relationship of mean effective stress and sonic interval velocity shows a better matched with the well data. All wells with both direct and indirect well pressure measurement in the study area were tested. Pore pressure prediction of Dukuh-1 and MDA-2 wells as the examples shows pore pressure slightly higher than the MW used during drilling in the deeper part of the well and in Dukuh-1 well closely follows the S_v (Figure 18).

The magnitude of the mean stress in both wells indicates sufficient mean effective stress to hold the MW from breaking the formation.

The MW used in the deeper part of Dukuh-1 well is less than the S_v . This is understandable to avoid the well breaking the formation. However, the information during drilling indicates many holes problems such as well flows and well kicks which is a sign of underbalance drilling. This is a good example where previous pre-drill pore pressure prediction may be built with only overburden or vertical stress as the main inducing agent without considering the compressional tectonic stress regime of the area. In the compressional tectonic setting, pore pressure prediction needs to take into account the three-dimensional nature of the stress field.

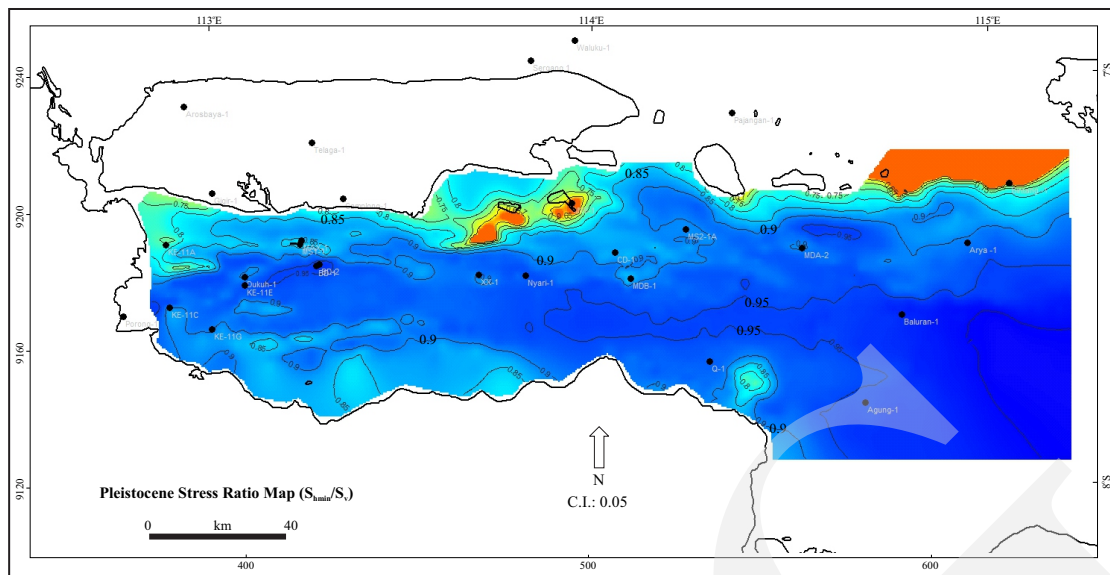


Figure 16. Ratio between minimum horizontal stress and vertical stress map is < 1 which suggest minimum horizontal stress as the minimum principle stress (S_3).

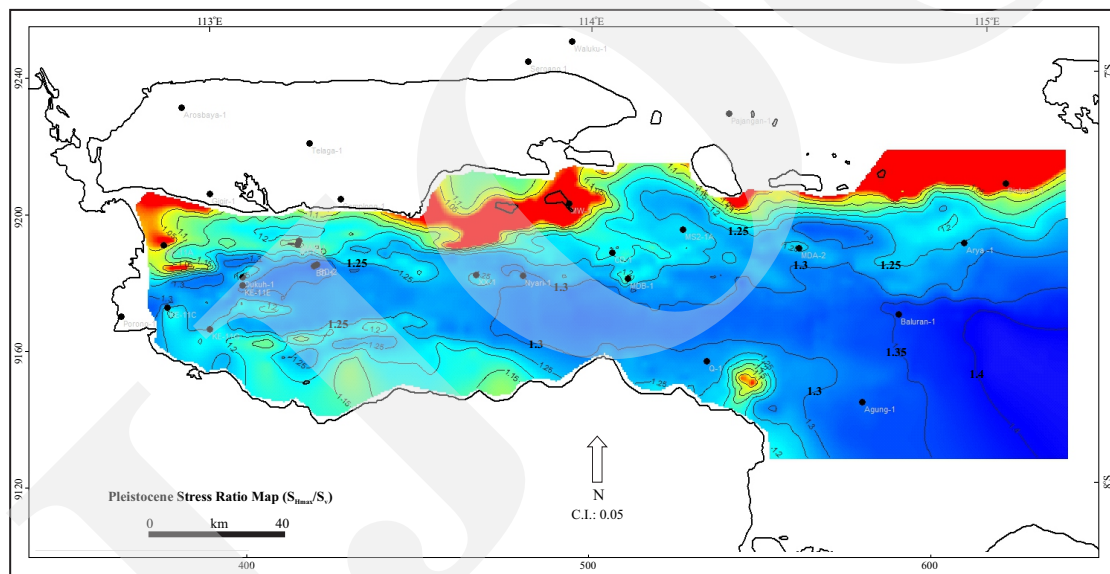


Figure 17. Ratio between maximum horizontal stress and vertical stress map is > 1 which suggest maximum horizontal stress as the maximum principle stress (S_1).

This case further implies that the new pore pressure prediction method manages to explain drilling problems and proves to work accurately in compressional tectonic setting. It is important to note that the effect of unloading processes such as hydrocarbon generation (Ramdhan and Goulty, 2011) and transformation of clay mineral smectite to illite (Goulty and Ramdhan, 2012) are considered minor to none in estimating pore pressure in the study area.

The pore pressure map was generated for the Pleistocene horizon by subtracting the mean stress distribution map with the mean effective stress distribution map (Figure 19). The pore pressure distribution of the Pleistocene horizon follows the structural trend. The lowest pore pressure magnitude is located in the northern and southern side of the study area. The pore pressure prediction distribution in the middle part of the study area forms a west to east elongated trend and is

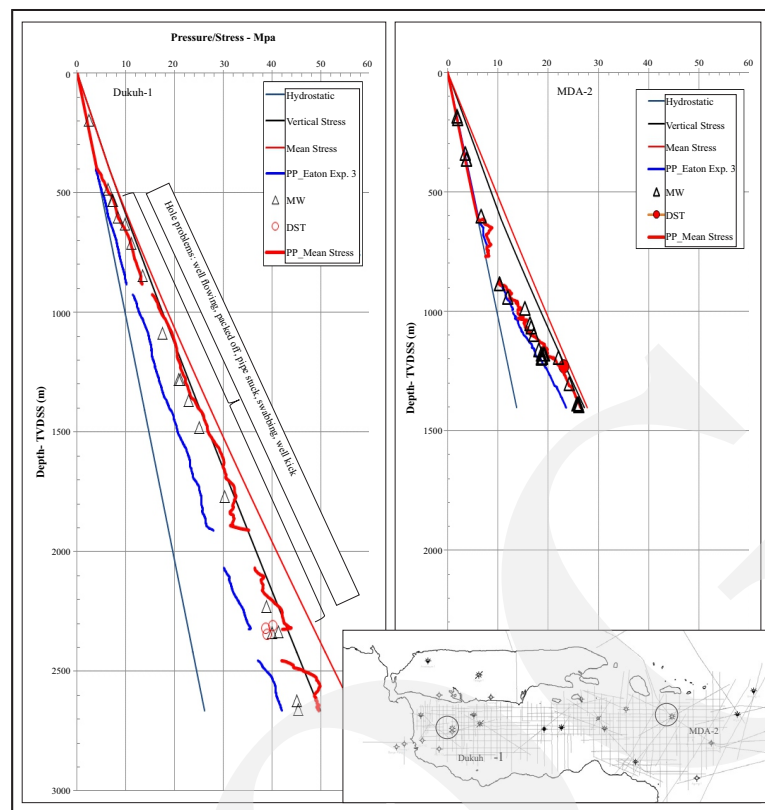


Figure 18. The new pore pressure prediction workflow proves to work in the studied area as shown in the two example wells: Dukuh-1 and MDA-2 wells. The normally used pore pressure prediction with standard exponential value of 3 (blue line) in both wells underestimate the well direct and indirect pressure measurements (DST and MW). Dukuh-1 well demonstrates many hole problems during drilling that may relate to under balance drilling from depth approximately 500 m TVDSS such as well flowing, packed off, stuck pipe, swabbing to well kicks. As discussed, the studied area is located in a compressional tectonic setting. Therefore, the pore pressure prediction workflow needs to accommodate the three principal stresses in a form of mean stress as the compaction main inducing agent. The new pore pressure prediction (red line) shows a slightly higher magnitude than the mud weight used in the Dukuh-1 well which explain why the well was in a continuous hole problems during drilling. Another example, the MDA-2 well illustrates the new workflow in pore pressure prediction generates a better match (red line) with the well data.

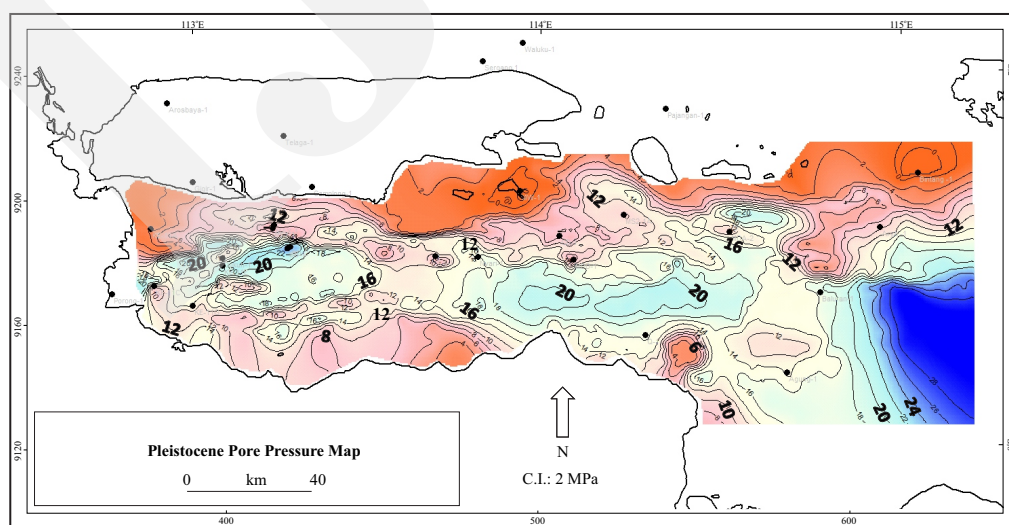


Figure 19. Pleistocene horizon pore pressure distribution generally follows the structure. The magnitude ranges from ≥ 0 MPa where the horizon basically exposed in Madura Island and the northern part (red) to magnitude > 26 MPa in eastern part of the studied area which is a structurally low area (dark blue).

divided into three high pressure areas. The highest pore pressure is located in the eastern part of the study area, in the structurally lowest area for the Pleistocene.

CONCLUSION

The new workflow in pore pressure prediction discussed in this paper takes into account the three-dimensional nature of the stress field for the compressional tectonic setting. It accommodates the three principal stresses, *i.e.* vertical stress, maximum horizontal stress, and minimum horizontal stress in a form of mean stress as the compaction main inducing agent. The application of this new workflow in well cases has resulted in a more accurate pore pressure prediction that will benefit drilling operation in preventing major incident such as blowouts. In Dukuh-1 well, as an example, the pore pressure prediction generated from the new work flow is able to explain the continuous hole problems such as well flows and well kicks that were recorded during drilling. In MDA-2 well, the new pore pressure prediction closely matches the well data, while the pore pressure prediction were generated using only overburden or vertical stress as the compaction main inducing agent underestimates the well data. A more accurate pore pressure prediction map has been generated to aid both hydrocarbon exploration and development activities in the study area.

ACKNOWLEDGMENTS

The authors would like to give a special acknowledgement to The Indonesian Government, specifically Data and Information Centre of the Ministry Energy and Mineral Resources (PUS-DATIN Kementerian ESDM) for their support and permission to use the data. Appreciation also goes to colleagues who have helped shaping this work.

REFERENCES

- Anderson, E.M., 1951. *The Dynamics of faulting and dyke formation with applications to Britain - 2nd edition*. Edinburgh, Oliver and Boyd. DOI: 10.1017/S0016756800065493.
- Bell, J.S., 1996. In situ stresses in sedimentary rocks (part 1): measurement techniques, *Geoscience Canada. Petro Geoscience*, 23, p.85-100. DOI: <https://journals.lib.unb.ca/index.php/GC/article/view/3910>.
- Bemmelen, R.W. van, 1949. *The Geology of Indonesia*, Government Printing Office, Nijhoff, The Hague, 1 A, 732pp.
- Brandsen, P.J.E. and Matthews, S.J., 1992. Structural and stratigraphic evolution of the East Java Sea, Indonesia. *Proceedings of Indonesian Petroleum Association, 21st Annual Convention*, p.417-453.
- Byerlee, J.D., 1978. Friction of rock. *Pure and Applied Geophysics*, 116, p.615-626. DOI: 10.1007/BF00876528.
- Eaton, B., 1975. The equation for geopressure prediction from well logs. *Society of Petroleum Engineers of AIME, SPE, Paper No. 5544*, 11pp. DOI: 10.2118/5544-MS.
- Engelder, T., 1993. *Stress regimes in the lithosphere*. Princeton, Princeton University Press, 457pp.
- Gardner, G.H F., Gardner, L.W., and Gregory, A.R., 1974. Formation velocity and density—the diagnostic basics for stratigraphic traps. *Geophysics*, 39, p.770-780. DOI: 10.1190/1.1440465.
- Genevraye, P.D. and Samuel, L., 1972. Geology of the Kendeng Zone. *Proceedings of Indonesian Petroleum Association*, 1, p.17-30.
- Goult, N.R., 1998. Relationships between porosity and effective stress in shales. *First Break*, 16, p.413. DOI: 10.1046/j.1365-2397.1998.00698.x.
- Goult, N.R. and Ramdhan, A.M., 2012. The challenge of pore pressure estimation in diagenetically consolidated mudrocks. *First Break*, 30, p.67-72. DOI: 10.3997/1365-2397.30.12.65618.

- Harrold, T.W.D., Swarbrick, R.E., and Goult, N.R., 1999. Pore pressure estimation from mudrock porosities in Tertiary basins, South-east Asia. *AAPG Bulletin*, 83 (7), p.1057-1067.
- Heidbach, Oliver, Rajabi, Mojtaba, Reiter, Karsten, Ziegler, Moritz, and WSM Team, 2016. *World Stress Map Database Release 2016*. 1(1). GFZ Data Services. DOI: 10.5880/WSM.2016.001.
- Hutasoit, L.M. and Ramdhan, A.M., 2014. Similarities of overpressuring in some Western Indonesia's sedimentary basin. *Proceedings of Indonesian Petroleum Association, 38th Annual Convention*, IPA14-G-356.
- Jaeger, J.C., Cook, N.G.W., and Zimmerman R.W., 2007. *Fundamentals of rock mechanics - 4th edition*, Blackwell Publishing, USA-UK-Australia, 489pp.
- Kusumastuti, A., Darmoyo, A.B., Suwarlan, W., and Sosromihardjo, S.P.C., 1999. The Wunut Field: Pleistocene volcanoclastic gas sands in East Java. *Proceedings of Indonesian Petroleum Association, 27th Annual Convention*, p.1-21.
- Magee, T., Buchan, C., and Prosser J., 2010. The Kujung Formation in Kurnia-1: A viable fractured reservoir play in the South Madura Block. *Proceedings of Indonesian Petroleum Association, 34th Annual Convention*, IPA10-G-005.
- Manik, P. and Soedaldjo, P.A., 1984. Prediction of abnormal pressure based on seismic data: A case study of exploratory well drilling in Pertamina UEP I AND UEP II work areas. *Proceedings of Indonesian Petroleum Association, 13th Annual Convention*, p.461-505.
- Metcalf, I., 2013. Gondwana dispersion and Asian accretion: Tectonic and palaeogeographic evolution of eastern Tethys. *Journal of Asian Earth Sciences*, 66, p.1-33. DOI: 10.1016/j.jseaes.2012.12.020.
- Pertamina BPPKA., 1996. *Petroleum geology of Indonesian Basins: Principles, methods, and applications, Volume IV: East Java Basin*. Jakarta, Pertamina BPPKA (Foreign Contractors Venture Development Body).
- Ramdhan, A.M. and Goult, N.R., 2011. Overpressure and mudrock compaction in the Lower Kutai Basin, Indonesia: A radical reappraisal. *AAPG Bulletin*, 95, p.1725-1744. DOI: 10.1306/02221110094.
- Ramdhan, A.M., Goult, N.R., and Hutasoit, L.M., 2011. The challenge of pore-pressure prediction in Indonesia's warm Neogene basins. *Proceedings of Indonesian Petroleum Association, 35th Annual Convention*, IPA11-G-141.
- Ramdhan, A.M., Hakim, F., Hutasoit, L.M., Goult, N.R., Sadirsan, W., Arifin, M., Bahesti, F., Endarmoyo, K., Firmansyah, R., Zainal, R.M., Gulo, M.Y., Sihman, M., Suseno, P.H., and Purwanto A.H., 2013. Importance of understanding geology in overpressure prediction: The example of the East Java Basin. *Proceedings of Indonesian Petroleum Association, 37th Annual Convention*, IPA13-G-152.
- Ratman N., Suwarta, T., and Samodra, H., 1998. *Geological Map of Indonesia, Surabaya Sheet, scale 1:100.000*. Geological Research and Development Centre.
- Ruth, P., Hillis, R., Tingate, P., Swarbrick, R., 2003. The origin of overpressure in 'old' sedimentary basins: An example from the Cooper Basin, Australia. *Geofluids*, 3, p.125-131. DOI: 10.1046/j.1468-8123.2003.00055.x.
- Ruth, P., Hillis R., Swarbrick, R., and Tingate, P., 2000. Mud weights, transient pressure tests, and the distribution of overpressure in the North West Shelf, Australia. *Petroleum Exploration Society of Australia Journal*, 28, p.59-66.
- Satyana, A.H., Erwanto, E., and Prasetyadi, C., 2004. Rembang-Madura-Kangean-Sakala (RMKS) fault zones, East Java Basin: The origin and nature of a geologic border. *Proceedings of Indonesian Association of Geologists, 33rd Annual Convention*, 23pp.
- Schutjens, P.M.T.M., Hanssen, T.H., Merour, J., de Bree, P., Coremans, J.W.A., and Helliesen, G., 2004. Compaction-induced porosity/permeability reduction in sandstone reservoirs: data and model for elasticity-dominated

- deformation. *SPE Reservoir Evaluation and Engineering*, June, 7 (3), 15pp.
- Sribudiyani, Muchsin, N., Ryacudu, R., Kunto, T., Astono, P., Prasetya, I., Sapiie, B., Asikin, S., Harsolumakso A.H., and Yulianto, I., 2003. The collision of the East Java microplate and its implication for hydrocarbon occurrences in the East Java Basin. *Proceedings of Indonesian Petroleum Association, 29th Annual Convention*, p.1-12.
- Tanikawa, W., Sakaguchi, M., Wibowo, H.T., Shimamoto, T., and Tadaï, O., 2010. Fluid transport properties and estimation of overpressure at the Lusi mud volcano, East Java Basin. *Engineering Geology*, 116, p.73-85. DOI: 10.1016/j.enggeo.2010.07.008.
- Terzaghi, K., 1925. *Principles of soil mechanics*. Engineering News-Record, 95, p.19-27.
- Tingay, M.R.P., 2003. *In situ stress and overpressures of Brunei Darussalam*, Ph. D. Dissertation, The University of Adelaide.
- Tingay, M.R.P., 2015. Initial pore pressures under the Lusi mud volcano, Indonesia. *Interpretation*, February, p.1-17. DOI: 10.1190/INT-2014-0092.1.
- Traugott, M., 1997. *Pore pressure and fracture pressure determination in deep water*, Deep Water Technology Supplement to World Oil, 8pp.
- Yassir, N.A. and Zerwer, A., 1997. Stress regimes in the Gulf Coast, offshore Louisiana from wellbore breakout analysis. *AAPG Bulletin*, 81(2), p.293-307.
- Yassir, N. and Addis, M.A., 2002. Relationships between pore pressure and stress in different tectonic settings, In: Huffman, A.R. and Bowers, G.L. (eds.), Pressure regimes in sedimentary basins and their prediction. *AAPG Memoir*, 76, p.79-88.
- Zahirovic, S., Seton, M., and Müller, R.D., 2014. The Cretaceous and Cenozoic tectonic evolution of Southeast Asia. *Solid Earth*, 5, p.227-273. DOI: 10.5194/se-5-227-2014, 2014.
- Zoback, M.D., 2007. *Reservoir geomechanics*. Cambridge University Press, New York, 505pp. DOI: 10.1017/CBO9780511586477.